Surfactant-induced flow compromises determination of air-water interfacial areas by surfactant miscible-displacement

Molly S. Costanza-Robinson, Ph.D.[*a] and Eric J. Henry, Ph.D.[b]

[a] Middlebury College, Program for Environmental Studies and Department of Chemistry & Biochemistry, 276 Bicentennial Way, Middlebury, VT 05753, USA

mcostanz@middlebury.edu

[b] University of North Carolina–Wilmington, Department of Geography and Geology, 601 South College Road, Wilmington, NC 28403, USA

ericjhenry5@gmail.com

*corresponding author

Submitted for consideration to *Chemosphere*
October 11, 2016
Revised
December 15, 2016

Running Title: Surfactant-induced flow compromises A_I determination by surfactant miscible-displacement

Keywords: *air-water interfacial area, surfactant-induced flow, modeling, unsaturated flow, tracer tests*

This work was funded by grants provided by the National Science Foundation (NSF), the Petroleum Research Fund, and Middlebury College.

Abstract

Surfactant miscible-displacement (SMD) column experiments are used to measure air-water interfacial area (A_I) in unsaturated porous media, a property that influences solute transport and phase-partitioning. The conventional SMD experiment results in surface tension gradients that can cause water redistribution and/or net drainage of water from the system ("surfactant-induced flow"), violating theoretical foundations of the method. Nevertheless, the SMD technique is still used, and some suggest that experimental observations of surfactant-induced flow represent an artifact of improper control of boundary conditions. In this work, we used numerical modeling, for which boundary conditions can be perfectly controlled, to evaluate this suggestion. We also examined the magnitude of surfactant-induced flow and its impact on A_I estimation during multiple SMD flow scenarios. Simulations of the conventional SMD experiment showed substantial surfactant-induced flow and consequent drainage of water from the column (e.g., from 75% to 55% S_W) and increases in actual A_I of up to 43%. Neither horizontal column orientation nor alternative boundary conditions resolved surfactant-induced flow issues. Even for simulated flow scenarios that avoided surfactant-induced drainage of the column, substantial surfactant-induced internal water redistribution occurred and was sufficient to alter surfactant transport, resulting in up to 23% overestimation of A_I. Depending on the specific simulated flow scenario and data analysis assumptions used, estimated A_I varied by nearly 40% and deviated up to 36% from the system's initial A_I. We recommend methods for A_I determination that avoid generation of surface-tension gradients and urge caution when relying on absolute A_I values measured via SMD.

INTRODUCTION

Accurate measurement of the air-water interfacial area (A_I) is important because A_I influences the accumulation of surface-active solutes at the air-water interface (AWI), solute- and particle transport in unsaturated systems, and mass-transfer kinetics of solutes across the AWI. A_I is commonly measured using laboratory-scale unsaturated surfactant miscible-displacement (SMD) experiments in which the accumulation of a surfactant tracer at the AWI retards its transport relative to a non-reactive tracer. The processes considered to affect the total retardation factor, R_T (-), of the interfacial tracer are shown in Eqn. [1] (Kim et al. 1997,1999):

$$R_T = 1 + \frac{\rho_b K_D}{\theta_W} + \frac{A_I K_{IW}}{\theta_W} \qquad [1]$$

where, ρ_b is porous medium bulk density (g cm^{-3}); θ_W is volumetric water content (-); K_D is the solid-phase sorption coefficient (cm^3 g^{-1}); and K_{IW} is the interfacial accumulation coefficient (cm). A_I used here and throughout refers to the area of the total air-water interface (i.e., area associated with water held via both film adsorption and capillarity), defined as the interfacial area per unit system volume (cm^2 cm^{-3} = cm^{-1}). As shown in Eqn. [1], R_T is a function of A_I, thereby allowing A_I to be estimated for a system with steady flow and constant θ_W if R_T and the remaining variables in Eqn. [1] are known.

The R_T necessary for use in Eqn. [1] is typically determined using tracer breakthrough curves as the ratio of the average travel time of the interfacial tracer, a surfactant, to that of a non-reactive tracer:

$$R_T = \frac{t_{\text{surfactant}}}{t_{\text{non-reactive}}} = 1 + R_S + R_I \qquad [2]$$

where, $t_{\text{surfactant}}$ and $t_{\text{non-reactive}}$ are the average travel times for the surfactant and non-reactive tracer pulses. The terms R_S and R_I represent the surfactant retardation due to sorption to the solid and accumulation at the AWI and correspond to the terms on the RHS of Eqn. [1], subject to the assumptions of steady flow and constant θ_W. A body of work has demonstrated, however, that surfactants can affect unsaturated flow, including by inducing non-steady flow and drainage (e.g., see review (Henry and Smith 2003)). Such disruptions to flow would influence solute transport and thereby measured R_T (Eqn. [2]) and A_I (Eqn. [1]).

The primary effect of surfactants on unsaturated flow is due to the dependence of soil-water pressure head, ψ (cm), on surface tension, σ (mN m^{-1}):

$$\psi = -\frac{2\sigma \cos\gamma}{\rho_w g r} \qquad [3]$$

where ρ_w is the solution density (g cm^{-3}); g is the gravitational acceleration (m s^{-2}); γ is the contact angle, assumed zero herein (Kibbey and Chen 2012, Tokunaga et al. 2004); and r is the radius of an equivalent cylinder (m). For example, at concentrations typically used in SMD experiments (0.05-2 mM), the surface tension of the conventionally used surfactant, sodium dodecyl benzene sulfonate (SDBS) is 43-57 mN m^{-1}, compared to the surface tension of pure water which is ~72 mN m^{-1} (Costanza-Robinson et al. 2012, Kim et al. 1997). The impact of concentration-dependent surface tension depression manifests as a shift in the moisture content-pressure head relationship (Karagunduz et al. 2001). As shown in Fig. 1, at moisture contents less than saturation, the pressure head in a surfactant-wetted medium is higher (less negative) than in the water-wetted medium (Henry and Smith 2003). Because pressure head gradients drive flow from regions of higher pressure toward regions of lower pressure, there is a tendency for water to flow from surfactant-containing regions (lower σ, higher ψ) toward surfactant-free regions (higher σ, lower ψ). Considerable variation in surfactant concentration can occur over short distances (i.e., the length of a solute front), resulting in pressure head gradients that can induce flow.

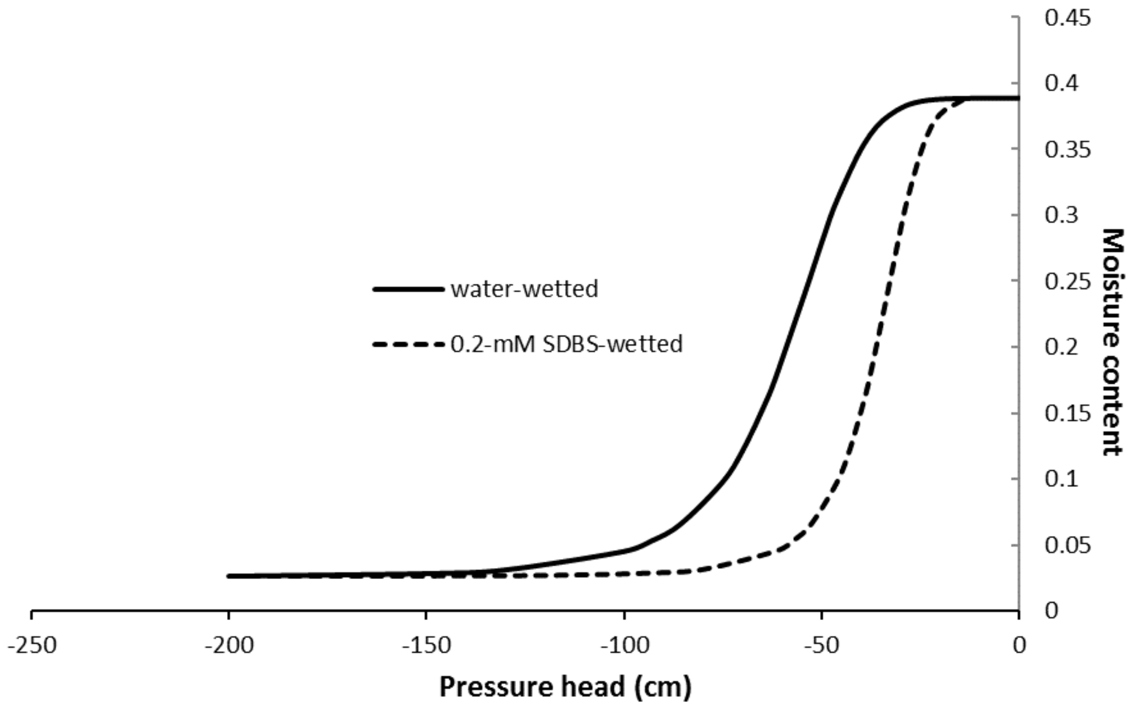

Figure 1. Soil water characteristic curves for pure-water wetted and surfactant-wetted sand.

The potential for surfactant-induced flow to affect conventional SMD experiments, and thereby A_I measurement, is recognized (Brusseau et al. 2015, Karagunduz et al. 2015, Kibbey and Chen 2012, Kim et al. 1997). Costanza-Robinson et al. (2012) found that as the surfactant (SDBS) pulse displaced resident water within the column, 24-51%, depending on influent SDBS concentration, of the water drained from the column. This drainage was associated with transient effluent flowrates of up to 27% above the steady-state conditions that existed prior to the surfactant introduction and 300% variation in estimated A_I, depending on how the drainage was accommodated in the data analysis. Studies utilizing surfactants for A_I determination by methods other than SMD, as well as unsaturated SMD experiments unrelated to A_I determination report similar surfactant-induced drainage (Bashir et al. 2011, Chen and Kibbey 2006, Karagunduz et al. 2015, Smith and Gillham 1999, Zartman and Barsch 1990). While use of lower surfactant concentrations reduces the magnitude of surfactant-induced flow (Chen and Kibbey 2006, Zartman and Barsch 1990), even low concentrations (e.g., 0.05 mM) can induce substantial surfactant-induced flow and drainage (Costanza-Robinson et al. 2012). Such surfactant-induced drainage represents non-steady flow and a non-constant θ_W, violating basic assumptions of the SMD method.

Surfactant effects, typically measured as net drainage from the system, have not been observed in all experimental systems, however. Brusseau et al. (Brusseau et al. 2007, 2015) only observed surfactant-induced drainage when using a hanging water column and not when using a vacuum chamber. They suggested that the strong vacuum control of the vacuum chamber prevents surfactant-induced drainage from occurring, even as others have observed surfactant-induced drainage when utilizing a vacuum chamber (Karagunduz et al. 2015). No explanation was provided regarding why a hanging water column should offer any less experimental control, nor for why a vacuum chamber should render the system immune to the uncontested physical basis for surfactant-induced drainage. Even so, it is worthwhile to examine this possibility because SMD is the principle experimental method used to measure air-water interfacial areas and is often used as the benchmark against which alternative methods are compared (e.g., Araujo et al. 2015).

In this work, we evaluated the suggestion that surfactant-induced effects can be avoided during SMD experiments by proper control of boundary conditions. We used a numerical flow and transport model that had been modified previously to include concentration-dependent effects of surface tension and surface tension gradients on unsaturated flow (Henry et al. 2001, 2002). In the present work, we further added the capability to account for surfactant accumulation at the AWI. Our SMD simulations are significant, because although the potential for surfactant-induced flow to occur and to influence the AWI and A_I measurement is regularly discussed, few studies have actually investigated the nature and magnitude of its influence on A_I measurement. Our simulations allowed us to investigate the reliability of available experimental SMD A_I estimates and provide recommendations for how these estimates might best be considered and used. Finally, we assessed whether minor changes to the conventional SMD experiment, including alternative boundary conditions and column orientation, are capable of resolving surfactant-induced flow issues. A benefit of simulating alternative boundary conditions was that they created a variety of surfactant-induced in-column behaviors and allowed us to probe their impact on SMD-estimated A_I.

Both air-water and NAPL-water experiments may involve surfactants and are often referred to using similar “wetting/non-wetting” terminology; nevertheless, these types of experiments differ markedly with regard to the unsaturated versus saturated nature of the flow, as well as to factors that influence the development of surface tension gradients. SMD experiments in unsaturated air-water systems are the subject of the current work; saturated NAPL-water experiments are not addressed.

METHODS

Numerical Model

HYDRUS 1D is a commonly used unsaturated flow and transport model (e.g., Simunek et al. 2016), but it does not account for surface tension effects on unsaturated flow nor for the process of solute accumulation at the AWI (Simunek et al. 1988). Henry and colleagues (Henry et al. 2001, 2002) previously modified HYDRUS 1D to include the effects of concentration-dependent surface tension on unsaturated flow and validated the model by comparison to surfactant-induced flow experiments. For the concentration-surface tension relationship, experimental surface tension-concentration data for SDBS (Costanza-Robinson et al. 2012) were fit with the relationship (Adamson and Gast 1997):

$$\frac{\sigma}{\sigma_0} = 1 - b\ln\left(\frac{c}{a} + 1\right) \qquad [4]$$

where a and b are compound-specific constants (for SDBS, a = 0.028 mM; b = 0.106); σ and σ_0 are the surface tensions at concentration c and the reference concentration (c_0) (σ_0 = 72 mN m^{-1} at c_0 = 0 mM SDBS), respectively.

HYDRUS 1D was further modified in the current work to incorporate the process of surfactant accumulation at the AWI. We took advantage of the fact that the model incorporates partitioning of volatile solutes between the bulk liquid and gas phases. Air-water interfacial partitioning is analogous to the bulk air-water process except that the concentration at the interface is a function of a different partitioning coefficient (K_{IW} instead of the Henry's coefficient) and the area of the AWI (A_I) rather than the volume of the gas phase. For the required model input of an A_I-S_W relationship, any reasonable model would suit the comparative purposes of the current work; we selected a relationship derived using X-ray computed microtomography, a surfactant-independent method, and that could be tailored to the surface area of the porous medium simulated here (Costanza-Robinson et al. 2008):

$$A_I = -1.6338 \times S_W + 163.41 \qquad [5]$$

Sorption of SDBS to the solid (K_D) and accumulation at the AWI (K_{IW}) were described using "effective" values (i.e., a single K value to represent a nonlinear isotherm) that correspond to the influent concentration for the surfactant pulses. Use of effective values yields an appropriate simulated travel time (Kim et al. 1997) that is internally consistent with subsequent data analysis, a point which we confirm in the results section below. Effective K_D values used were 0.063, 0.105, and 0.202 cm^3 g^{-1} for influent SDBS concentrations of 0.2, 0.1, and 0.05 mM, respectively; the associated effective K_{IW} values used were 0.0015, 0.0029, and 0.00582 cm (Costanza-Robinson et al. 2012).

The simulated column system was a soil column 10.7-cm long containing a sand with properties similar to that used by Costanza-Robinson et al. (2012) The commonly used van Genuchten-Mualem relationship is used in HYDRUS 1D to describe soil water retention (Fig. 1) and unsaturated hydraulic conductivity. Model parameters used were: saturation water content, θ_S = 0.39; residual water content, θ_R = 0.03; van Genuchten fitting parameters, α = 0.01801 cm^{-1} and n = 5.92667; saturated hydraulic conductivity, K_S = 0.03155 cm min^{-1}; ρ_b = 1.6 g cm^{-3}; and longitudinal dispersivity, α_L = 1.0 cm (Simunek et al. 1988). The model has an option to include hysteresis in the water retention functions, but Henry et al. (2002) reported difficulties using hysteresis in surfactant-induced flow modeling and to avoid those difficulties we did not include hysteresis in the current simulations. Other simulations of surfactant-influenced systems suggest that hysteresis exerts minimal impact on surfactant R_T (e.g., Fig. 3C and Table 2 in Karagunduz et al. 2015), and consequently, on A_I determination. In fact, R_T derived from simulations that excluded hysteresis matched experimentally measured values slightly better than those that included hysteresis. For these reasons, we are confident that our simulations provide a reasonable approximation of the system parameters we seek to evaluate.

Surfactant-Miscible Displacement Simulations

For most simulations, the physicochemical properties of a 0.2-mM SDBS solution were used for the simulated influent surfactant solution. This concentration represents the high end of those used experimentally, is below the critical micelle concentration (CMC_{SDBS} = ~3 mM (Hait et al. 2003)), and was expected to generate surfactant-induced flow; thus, this concentration provides an experimentally relevant and appropriate challenge with respect to studying and attempting to resolve surfactant effects. Properties of 0.1 and 0.05-mM SDBS solutions were used for select simulations to test system responses to lower surfactant concentration. Similarly, the water saturation (S_W, defined as θ_W/θ_S) was set to an initial value of 75% for most SMD simulations because the magnitude of surfactant-induced flow is expected to be larger in wetter systems than in drier systems (Costanza-Robinson et al. 2012). Select simulations of systems with initial S_W of 25 and 50% were also conducted.

All simulations began with steady flow of pure water under prescribed boundary conditions (Table 1) corresponding to the desired S_W, after which surfactant solution was applied under the same boundary conditions. Surfactant input continued until the influent (C_0) and effluent (C) surfactant concentration were equal (i.e., C/C_0 = 1). Average surfactant travel time ($t_{surfactant}$) was determined from simulated breakthrough curves as the time at which C/C_0 reached 0.5; $t_{non\text{-}reactive}$ was similarly determined from a separate (surfactant-free) simulation for a non-reactive tracer, using the same boundary conditions and column orientation as for the surfactant. Solute travel times were used to calculate R_T (Eqn. [2]) and therewith, A_I (Eqn. [1]).

Model testing

Because of the importance of accumulation at the AWI when examining surfactant transport, we added this capability to the HYDRUS 1D model. Because the simulations presented here are the first to include partitioning to the AWI in a model of surfactant-affected flow, it was important to test the ability of our modified model to correctly partition surfactant to the solid-water and air-water interfaces. We did so by comparing R_T calculated using simulated breakthrough curves (Eqn. [2]) to those calculated independently from prescribed initial system and SDBS physicochemical parameters (Eqn. [1]). In the absence of surfactant-induced flow, Eqns. [1] and [2] should yield the same value for R_T. In contrast, because surfactant-induced flow can cause non-steady tracer flux and changes in water content over the course of the simulated experiment, it cannot be assumed that Eqns. [1] and [2] would yield the same R_T for a system experiencing surfactant-induced flow effects. For this reason, model test simulations excluded surface tension effects on flow, but in all other respects utilized boundary condition and flow parameters that were identical to our baseline simulation (Scenario A, described below), which reflects the conventional SMD experiment. Test simulations were conducted for cases that included surfactant partitioning to the solid only (K_D partitioning); partitioning to the AWI only (K_{IW} partitioning); or partitioning to both solid and AWI (K_D and K_{IW} partitioning).

The test simulations were also used to evaluate the model performance with regard to A_I estimation. Under the steady flow conditions used in the test simulations, θ_W, S_W, and A_I are constant and uniform in the column, such that A_I calculated using breakthrough curves (Eqn. [2]) should match the true values calculated for the initial S_W in the simulated (Eqn. [5]). These latter A_I values are referred to hereafter as "initial true" A_I, indicating that they are the A_I values the simulations should produce for the initial system if the model is functioning properly and if surfactant-induced flow is not influencing the simulated experiment.

SMD flow scenarios

The model was used to evaluate the occurrence and magnitude of surfactant-induced flow and drainage in four SMD scenarios (Table 1). In all scenarios, K_D and K_{IW} partitioning *as well as surfactant-induced flow* were included. The conventional setup for unsaturated SMD experiments is steady downward flow with a pump-controlled constant flux upper boundary and a constant head lower boundary controlled by a hanging water column or other pressure control apparatus (e.g., vacuum chamber) (Brusseau et al. 2007, 2015, Costanza-Robinson et al. 2012, Kim et al. 1997, Saripalli et al. 1997). The specific upper and lower boundary conditions are chosen to yield a unit hydraulic gradient, steady flow, and constant and uniform S_W (and A_I) within the column. Simulation of this conventional experimental setup is considered to be our "base" case, is referred to as Scenario A (downward constant flux at the upper boundary of 1.02 x10^{-2} cm/min and a constant head at the lower boundary of -48.8 cm). Scenarios B-D explored either unconventional column orientations or alternative boundary conditions to explore whether minor alterations to the conventional SMD experiment could reduce surfactant-induced flow or its impacts on A_I determination. Scenario D, in particular, allowed us to assess the effects on A_I determination of surfactant-induced *in-column water redistribution* (no net drainage of the system) separately from the effects of surfactant-induced *drainage*. For all scenarios, the simulated boundary conditions and initial system conditions were chosen to produce an initial flux, $S_{W,}$ and A_I that closely matched Scenario A.

Table 1. Simulation scenarios examined for their effect on surfactant-induced flow and A_I determination, including the conventional SMD setup (Scenario A) and alternative column orientation and column boundary conditions (BCs).

Scenario	Flow direction	Inlet BC	Outlet BC
A (base case)	downward	constant flux	constant head
B	downward	constant head	constant head
C	horizontal	constant head	constant head
D	downward	constant flux	constant flux

The first metric we used to assess the magnitude of surfactant-induced flow in the four scenarios was the change in column-averaged S_W within the simulated soil column as a function of time, as used by others to quantify surfactant-induced perturbations in their experimental systems (surfactant-induced drainage) (Brusseau et al. 2007, 2015, Costanza-Robinson et al. 2012). Monitoring drainage alone does not provide information about spatial variations in water content with respect to time within the column, however; thus, in some cases, we also assessed the surfactant-induced internal redistribution of water within the column. We refer to θ_W, rather than S_W, in some sections of the discussion below because it facilitates the interpretation of the results relative to the water characteristic curves (Fig. 1) and the symbology used in Eqn. [1].

RESULTS AND DISCUSSION

Model testing

To ensure that the modifications to the HYDRUS 1D model for surfactant accumulation at the AWI functioned properly, we conducted test simulations that included partitioning to the solid phase and/or to the AWI, but excluded surface tension effects on flow. The results of model test simulations are presented more fully in the Supplemental Information. Briefly, R_T and its sub-components determined based on the simulated breakthrough curves (Fig. SI-1) and Eqn. [2] matched those independently calculated using the surfactant and system parameters and Eqn. [1] over a range of initial S_W from 25-75%. The A_I values based on simulations also matched the initial true A_I prescribed by the model input relationship (Eqn. [5]) to within 0.3%. The agreement with respect to surfactant retention and A_I confirm that the modified model functions correctly with respect to surfactant partitioning. The model testing also confirms that in a system with steady flow the use of K_D and K_{IW} as "effective" parameters associated with the influent surfactant concentration is valid for determining R_T, and hence A_I, as noted by Kim et al. (1997). Results of the model test case that included both K_D and K_{IW} partitioning but excluded surfactant-induced flow serve as an important point of comparison for the simulated SMD flow scenario results presented below.

Surfactant-induced flow during SMD flow scenarios

Scenario A

Representative Scenario A simulation data for breakthrough curves and column-averaged S_W vs. time are shown in Fig. 2A and 2B, respectively, for a system initially at 75% S_W. As expected, SDBS transport is retarded relative to the non-reactive tracer, and SDBS retardation is inversely

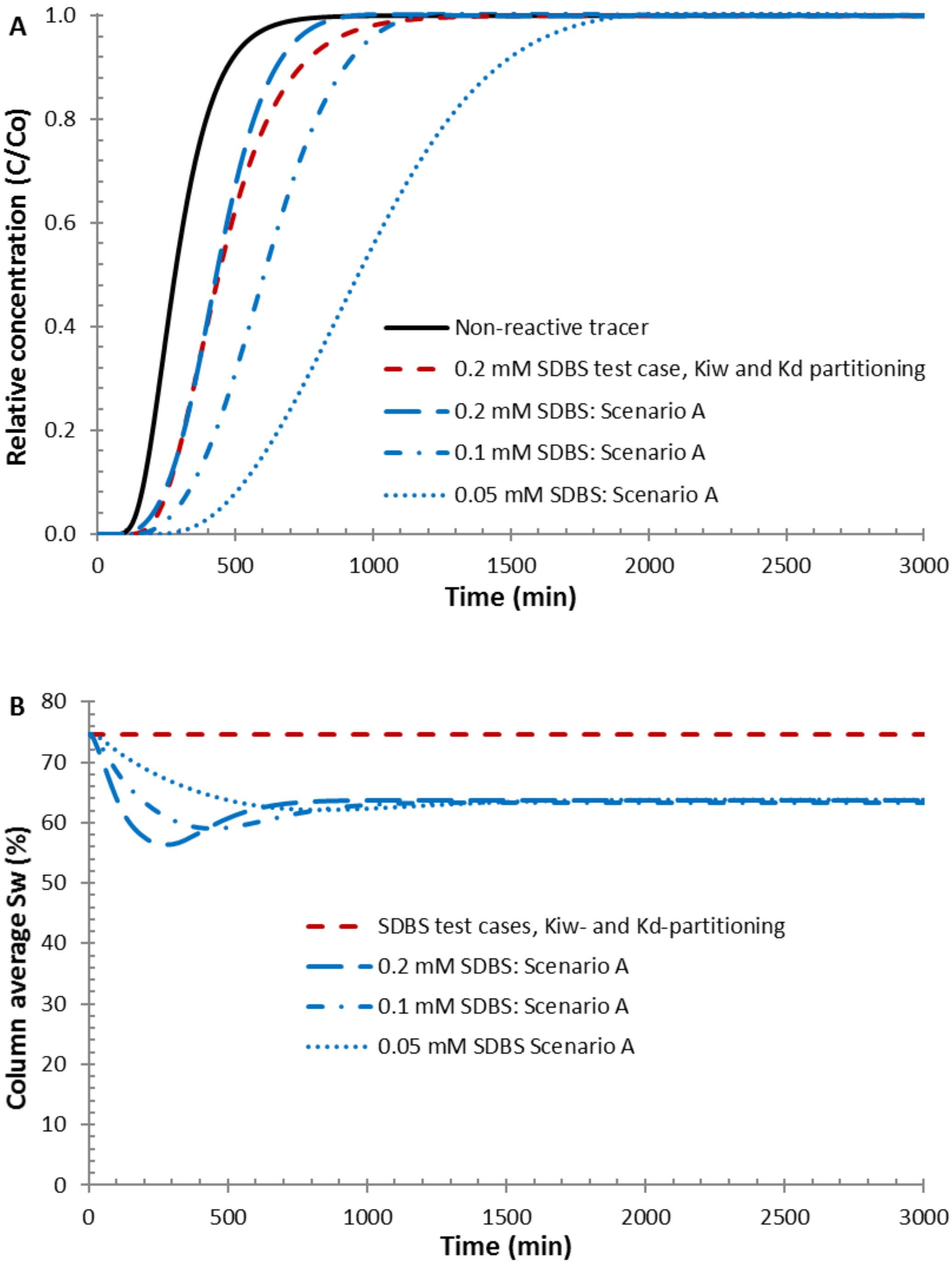

Figure 2. A) Simulated breakthrough curves and **B)** S_W-time relationships for Scenario A (blue in all figures) for systems at initial S_W of 75% and three influent SDBS concentrations. Breakthrough results for the non-reactive tracer (black) and the 0.2 mM SDBS K_D and K_{IW} partitioning test case (red), which do not include surfactant-induced flow, are included for comparison.

proportional to input concentration due to the inverse relation between concentration and both K_D and K_{IW}. The effect of surfactant-induced flow on the transport of SDBS is shown for the 0.2 mM SDBS input concentration, whereby SDBS travel time is slightly decreased in Scenario A as compared to the (K_D and K_{IW} partitioning) model test simulation. Fig. 2B shows that as surfactant solution displaces water in the column, a rapid decrease in S_W is induced that is proportional in magnitude to the influent SDBS concentration, followed by a modest rewetting. This surfactant-induced drainage is consistent with the enhanced SDBS transport through the column observed and also with both SMD experiments for A_I determination that utilized hanging water columns (Brusseau et al. 2015, Costanza-Robinson et al. 2012) and other simulations and experiments unrelated to A_I determination (Bashir et al. 2011, Chen and Kibbey 2006, Henry et al. 2002, Karagunduz et al. 2015, Smith and Gillham 1999, Zartman and Barsch 1990).

Scenarios B and C

Unconventional flow scenarios allowed us to examine whether minor modifications to the (simulated) experimental setup might be employed to minimize the magnitude or impact on estimated A_I of surfactant-induced flow. The breakthrough curves and S_W vs. time simulation results, respectively, for Scenarios B and C are shown in Fig. 3A and 3B. In Scenarios B and C, the SDBS arrival wave is substantially delayed, with $C/C_0 = 0.5$ not yet achieved within the 8400 min simulation time (see Fig. 3A inset). This behavior is explained by the observed drainage of roughly half of the system water (Fig. 3B). Specifically, although the initial drainage pulse facilitates the transport of the surfactant toward the column outlet, under the substantially drained conditions the unsaturated hydraulic conductivity is also markedly reduced. This low

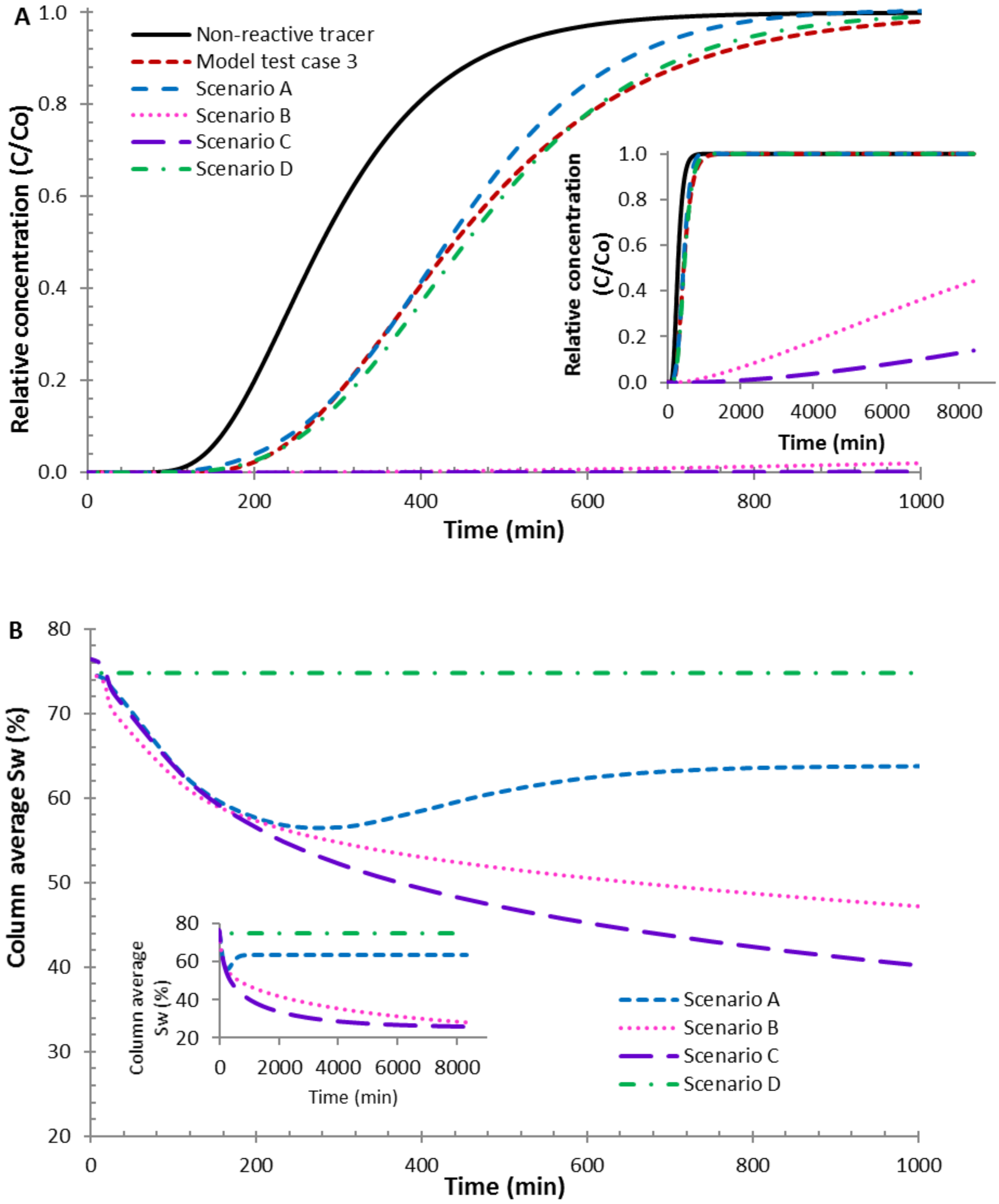

Figure 3. A) Simulated breakthrough curves and **B)** S_W-time relationships for SDBS under Scenarios A-D with an initial S_W of ~75% and influent SDBS concentration of 0.2 mM. Simulated breakthrough results for the non-reactive tracer (black) and the 0.2-mM SDBS K_D and K_{IW}-partitioning test case (red), which do not include surfactant-induced flow, are included for comparison. Insets show full simulation time.

conductivity reduces the rate at which water can be conveyed through the system (under constant head boundary conditions), slowing advance of the solute front. SDBS retardation is further enhanced via accumulation at the larger AWI that exists under the drained conditions.

The substantial drainage in Scenario B and C simulations is caused by the constant head boundary conditions used at the column inlet. At the pressure head of approximately -48.8 cm specified at the boundaries, the initial θ_W in the column was ~0.29 for the water-wetted medium (Fig. 1). As surfactant solution replaces pure water and the moisture relationship transitions from water-wetted behavior to surfactant-wetted behavior, the soil can hold less solution at a given pressure head. For example, although the sand had a θ_W of ~0.29 at a pressure head of -48.8 cm for the water-wetted sand, the θ_W at that same pressure head is ~0.04 when wetted with surfactant solution. This decrease in θ_W at the pressure head specified at the inlet boundary as surfactant entered the column resulted in a decrease in the flux at that boundary, further contributing to the drainage of the column (Smith and Gillham 1994). The substantial drainage and failure of SDBS to achieve $C/C_0 = 0.5$ for Scenarios B and C within the simulated time suggests that these boundary conditions will see limited practical application for A_I measurement, and also that R_T derived from such experiments would result in dramatically overestimated A_I.

Scenario D

The breakthrough curves and S_W vs. time simulation results for Scenario D are also shown in Fig. 3. The SDBS arrival is slightly delayed relative to the K_D and K_{IW} partitioning test case (which excludes surfactant-induced flow), even as the constant flux boundary conditions on both ends of the column mandate that column-averaged S_W remains constant. Simulated depth-profiles for θ_W, surfactant (relative) concentration, and pressure head for several simulation times allow us to examine Scenario D surfactant effects in more detail (Fig. 4). Prior to the application of the surfactant solution (i.e., t = 0 profiles), the entire column was at a steady state condition with $C/C_0 = 0$. The 30-min profiles show the surfactant input pulse near the top of the column (inlet), which increases pressure head (i.e., pressure head becomes less negative) due to the corresponding decrease in surface tension. The newly created surface tension (pressure head) gradient compels drainage near the inlet despite the fact that fluid was being applied at a constant rate. The drainage near the inlet decreases water content and unsaturated hydraulic conductivity at that location; however, the surfactant-affected pressure head gradient had also increased, which allows the porous medium to accommodate the constant flux despite the lower (local) conductivity. Meanwhile, the upper drainage resulted in the accumulation of liquid in the lower portion of the column, which cannot dissipate due to the constant flux lower boundary condition. These transient processes causing internal water redistribution under constant flux boundary conditions are consistent with previous modeling and experimental work related to surfactant-induced flow (Henry and Smith 2002, 2006, Henry et al. 2002, Karagunduz et al. 2015, Smith and Gillham 1994, 1999). As surfactant solution continued to be applied to the column, concentration gradients in the column eventually diminish, as do concentration-dependent pressure head gradients (e.g., 390-minute profiles), ultimately leading to a new steady-state condition (t = 1110-min profiles).

In summary, for Scenario D large localized variations in θ_W occur within the column during SDBS tracer application despite the fact that the constant flux boundary conditions require that the column-averaged S_W remains constant. We hypothesize that the behavior observed in

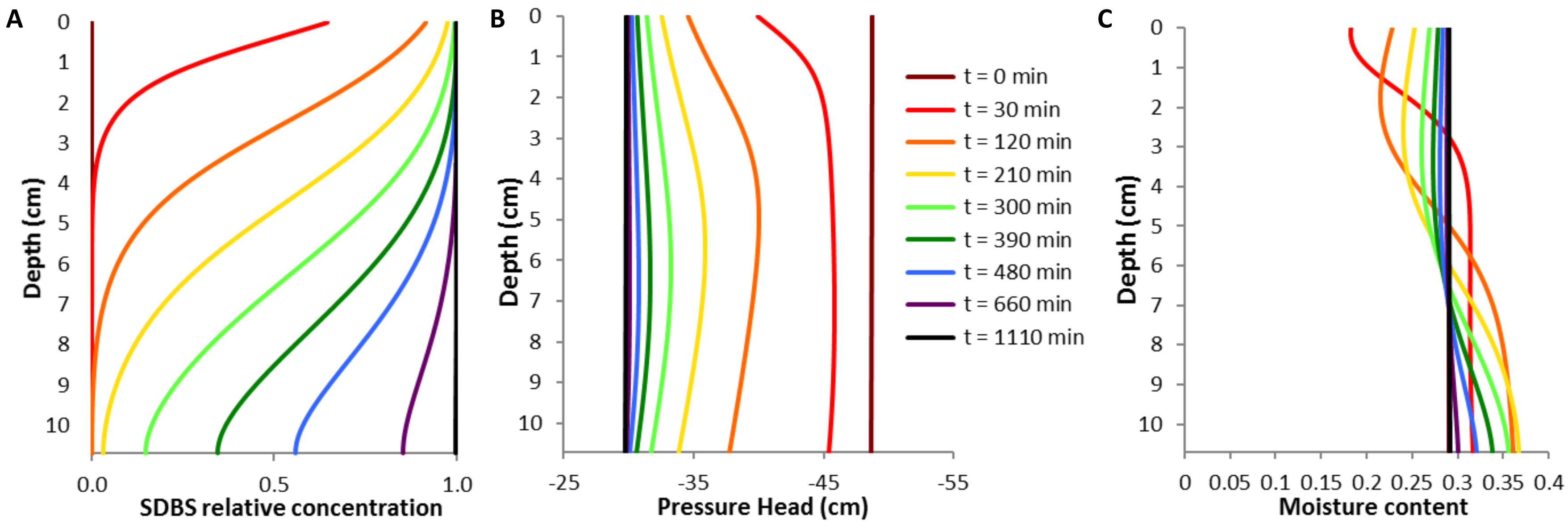

Figure 4. Simulated depth profiles for Scenario D of **A)** SDBS concentration; **B)** pressure head; and **C)** water content for multiple time points in a system at initial 75% S_W and 0.2 mM SDBS.

376

Scenario D provides a glimpse into the behavior that may be occurring in some SMD experiments in which surface tension gradients exist that should induce drainage, but for which no drainage is observed (Brusseau et al. 2007, 2015). Although the absence of net drainage in experimental systems has been interpreted as indicating that surfactant effects have been prevented and pose no problem for A_I measurement (Brusseau et al. 2015), our simulations suggest otherwise.

Effects on the AWI and A_I estimation during SMD flow scenarios

Because of the substantial surfactant-induced drainage and long solute travel times observed for Scenarios B and C, only Scenarios A and D appear as feasible experimental possibilities going forward. Thus, we focus on evaluating the impact of surfactant-induced flow on the AWI and A_I estimation for Scenarios A and D only.

Impact of surfactant-induced flow on the AWI

For the Scenario A simulations, drainage occurs over the course of surfactant-input, resulting in a final S_W of ~64% and an increase in the actual A_I in the simulated system of 59.3 cm^{-1} (Fig. 2B). This value is 43% higher than the initial true A_I of 41.4 cm^{-1} associated with the initial S_W of 75% (Eqn. 5), representing a substantial alteration to the AWI. For Scenario D, we can appraise the impact of surfactant-induced flow on the AWI by first considering the maximum and minimum θ_W within the column at a given time in Fig. 4C. For example, the t = 120-min profile has the largest range between the maximum and minimum θ_W. At the column location associated with the maximum θ_W (0.36), the corresponding local A_I would be 12.6 cm^{-1}. At the column location associated with the minimum θ_W (0.22), the corresponding local A_I would be 71.2 cm^{-1}. Despite the local changes to the AWI, microtomography-based A_I measurements on porous media columns with both uniform and non-uniform water distributions suggest that total column-averaged A_I depends linearly on column-averaged θ_W and is independent of the distribution of the water (Costanza-Robinson et al. 2011). Thus, so long as the column-averaged θ_W remains constant throughout the experiment, as it does in Scenario D, the actual column-averaged A_I should as well. While a constant actual A_I may appear promising, the goal of the SMD experiment is not only not to disrupt the initial column-average A_I, but rather to produce accurate A_I estimates; thus, in addition to evaluating the effect of surfactant-induced flow on the actual AWI, effects on estimated A_I must be considered.

Impact of surfactant-induced flow on estimated A_I

A_I is estimated using the simulated breakthrough curve data and Eqns. [2] and [1] and can be compared against values obtained independent of the simulations using Eqn. [5] and a representative column-averaged θ_W. In the standard SMD analysis, the initial θ_W (which is assumed to remain constant) is used. But given that surfactant-induced flow violates fundamental method assumptions, the theoretical justification for using initial θ_W (or final or time-averaged, for that matter) in Eqn. [1] is not clear. Nevertheless, if one ignores that substantial surfactant-induced flow has occurred, and the A_I is calculated using travel times and initial θ_W, we obtain the estimated A_I values presented in Table 2. Scenario A consistently underpredicts the initial true A_I, while Scenario D overpredicts it, findings that are consistent with the breakthrough curves in Fig. 3A. Estimated A_I for both simulation scenarios deviated further from the initial true A_I as initial S_W increased, consistent with the larger magnitude of surfactant-induced flow in wetter systems. At the highest initial S_W, estimated A_I values are 35.4 and 50.7 cm^{-1} for Scenarios

A and D, respectively, differing by -14% and +23% from the initial true A_I. Scenario D consistently yielded A_I worse estimates than Scenario A (14 ± 8% and 8 ± 5% error for Scenarios D and A, respectively). The smaller errors in measured A_I for Scenario A were surprising to us; we anticipated that the substantial surfactant-induced drainage and alterations to the AWI observed in Scenario A simulations would result in larger A_I estimation errors as compared to the less dramatic water redistribution-only observed in Scenario D. We conclude that even as the actual column-averaged A_I is unlikely to be changed by the internal water redistribution in Scenario D, that tracer transport is altered sufficiently to compromise estimated A_I.

Table 2. Comparison of initial true A_I with the estimated A_I derived from simulated breakthrough curves and initial S_W for Scenarios A and D (0.2 mM SDBS input), expressed as % error. Slight variations in the initial true A_I values for the two scenarios are due to differences in the types of boundary conditions utilized.

	A_I (cm^{-1})					
	Scenario A			**Scenario D**		
S_W	**Initial true**	**Simulated**	***Error (%)***	**Initial true**	**Simulated**	***Error (%)***
0.25	123.1	120.1	*-2.4*	122.9	128.5	*+4.6*
0.35	100.5	95.8	*-4.7*	99.2	106.9	*+7.8*
0.55	73.2	67.3	*-8.1*	72.7	83.8	*+15.3*
0.65	53.4	47.3	*-11.4*	52.6	63.5	*+20.7*
0.75	41.4	35.4	*-14.1*	41.2	50.7	*+23.1*

The generalizability of our simulation results to a variety of porous media systems has not yet been investigated, although experimental work suggests that surfactant-induced flow and A_I measurement errors would be larger for coarser porous media and for higher influent surfactant concentrations (Brusseau et al. 2015, Chen and Kibbey 2006, Costanza-Robinson et al. 2012).

Experimental SMD A_I estimates using initial θ_W generally conform to expected A_I-S_W trends, and thus, may well be correlated with initial true A_I; however, given the methodological complications suggested by our simulations, it is unclear what these estimate A_I values physically represent in an absolute sense. Moreover, our results suggest the possibility that experimental A_I estimates for the same porous media at the same initial S_W may differ by as much as 40%, depending on whether the experimental SMD setups allow for or preclude surfactant-induced net drainage of column moisture.

CONCLUSIONS

Simulation results for conventional SMD experiments (Scenario A) in which boundary conditions were held perfectly constant corroborate experimental work demonstrating surfactant-induced drainage to be an inherent consequence of the conventional experiment. Our simulations conform with theory and strongly suggest that surfactant-induced flow must occur when a constant head boundary condition is used at the outlet and a lower surface tension solution displaces a solution of higher surface tension. In the conventional SMD experiment, these processes likely result in underestimated A_I. Even in cases where net drainage from the column is somehow precluded, such as by constant flow boundary conditions (Scenario D), internal redistribution of column water appears to slow tracer transport and result in overestimated A_I. Thus, we caution that the absence of drainage in an experimental system should not be construed as absence of surfactant-induced flow, nor that A_I estimates are unaffected. Simple adjustments in column orientation or boundary conditions do not resolve the issues associated with surfactant-induced flow.

The current findings support a growing literature cataloguing the importance of surface tension gradients on unsaturated flow and that surfactant-induced methodological violations pose a distinct challenge to any absolute physical interpretation of resulting A_I estimates. If SMD is to be used, approaches for eliminating surface tension gradients, such as using a radiolabeled surfactant to displace its non-labeled analog and other similar approaches (Kim et al. 1997, Brusseau et al. 2015), are recommended. Alternatively, methods for A_I measurement might be used that do not rely on miscible displacement and avoid surfactant-induced flow effects (Chen and Kibbey 2006), or that avoid surfactants altogether (e.g., microtomographic imaging) (Brusseau et al. 2007, Chen et al. 2007, Culligan et al. 2004, Costanza-Robinson et al. 2008).

ACKNOWLEDGEMENTS

We are grateful to Dr. Jirka Simunek (University of California-Riverside) for sharing the HYDRUS 1D (FORTRAN) source code and to two anonymous reviewers for their constructive suggestions. The authors thank Mr. Emory Payne for assistance in making figures and proofing the manuscript. This work was funded by the National Science Foundation (EAR-0711499), the Petroleum Research Fund (47012-GB8), and Middlebury College.

REFERENCES

Adamson, A. W. and A. P. Gast (1997). Physical Chemistry of Surfaces. New York, John Wiley & Sons, Inc.

Araujo, J. B., J. Mainhagu and M. L. Brusseau (2015). "Measuring air-water interfacial area for soils using the mass balance surfactant-tracer method." Chemosphere **134**:199-202, DOI: 10.1016/j.chemosphere.2015.04.035.

Bashir, R., J. E. Smith and D. E. Stolle (2011). "The effect of ionic strength on surfactant-induced unsaturated flow." Can. Geotech. J. **48**:644.

Brusseau, M. L., A. El Ouni, J. B. Araujo and H. Zhong (2015). "Novel methods for measuring air-water interfacial area in unsaturated porous media." Chemosphere **127**:208-2013, DOI: 10.1016/j.chemosphere.2015.01.029.

Brusseau, M. L., S. Peng, G. Schnaar and A. Murao (2007). "Measuring air-water interfacial areas with X-ray microtomography and interfacial partitioning tracer tests." Environ. Sci. Technol. **41**:1956-1961.

Chen, D., L. J. Pyrak-Nolte, J. Griffin and N. J. Giordano (2007). "Measurement of interfacial area per volume for drainage and imbibition." Water Resour. Res. **43**:W12504, DOI: W12504, DOI: 10.1029/2007wr006021.

Chen, L. and T. C. G. Kibbey (2006). "Measurement of air-water interfacial area for multiple hysteretic drainage curves in an unsaturated fine sand." Langmuir **22**:6874-6880.

Costanza-Robinson, M. S., B. D. Estabrook and D. F. Fouhey (2011). "Representative elementary volume estimation for porosity, moisture saturation, and air-water interfacial areas in unsaturated porous media: Data quality implications." Water Resour. Res. **47**:W07513, DOI: 10.1029/2010WR009655.

Costanza-Robinson, M. S., K. H. Harrold and R. M. Lieb-Lappen (2008). "X-ray microtomography determination of air-water interfacial area-water saturation relationships in sandy porous media." Environ. Sci. Technol. **42**:2949-2956, DOI: 10.1021/es072080d.

Costanza-Robinson, M. S., Z. Zheng, E. J. Henry, B. D. Estabrook and M. H. Littlefield (2012). "Implications of surfactant-induced flow for miscible-displacement estimation of air-water interfacial areas in unsaturated porous media." Environ. Sci. Technol. **46**:11206-11212, DOI: 10.1021/es303003v.

Culligan, K. A., D. Wildenschild, B. S. B. Christensen, W. G. Gray, M. L. Rivers and A. F. B. Tompson (2004). "Interfacial area measurements for unsaturated flow through a porous medium." Water Resour. Res. **40**:W12413, DOI: 10.1029/2004wr003278.

Hait, S. K., P. R. Majhi, A. Blume and S. P. Moulik (2003). "A critical assessment of micellization of sodium dodecyl benzene sulfonate (SDBS) and its interaction with poly(vinyl pyrrolidone) and hydrophobically modified polymers, JR 400 and LM 200." J. Phys. Chem. B **107**:3650-3658, DOI: 10.1021/jp027379r.

Henry, E. J. and J. E. Smith (2002). "The effect of surface-active solutes on water flow and contaminant transport in variably saturated porous media with capillary fringe effects." J. Contam. Hydrol. **56**:247-270.

Henry, E. J. and J. E. Smith (2003). "Surfactant-induced flow phenomena in the vadose zone: A review of data and numerical modeling." Vadose Zone J. **2**:154-167, DOI: 10.2113/2.2.154.

Henry, E. J. and J. E. Smith (2006). "Numerical demonstration of surfactant concentration-dependent capillarity and viscosity effects on infiltration from a constant flux line source." J. Hydrol. **329**:63-74.

Henry, E. J., J. E. Smith and A. W. Warrick (2001). "Surfactant effects on unsaturated flow in porous media with hysteresis: Horizontal column experiments and numerical modeling." J. Hydrol. **245**:73-88.

Henry, E. J., J. E. Smith and A. W. Warrick (2002). "Two-dimensional modeling of flow and transport in the vadose zone with surfactant-induced flow." Water Resour. Res. **38**:1251, DOI: 10.1029/2001WR000674.

Karagunduz, A., K. D. Pennell and M. H. Young (2001). "Influence of a nonionic surfactant on the water retention properties of unsaturated soils." Soil Sci. Soc. Am. J. **65**:1392-1399.

Karagunduz, A., M. H. Young and K. D. Pennell (2015). "Influence of surfactants on unsaturated water flow and solute transport." Water Resour. Res. **51**:1977-1988, DOI: 10.1002/2014WR015845.

Kibbey, T. C. G. and L. Chen (2012). "A pore network model study of the fluid-fluid interfacial areas measured by dynamic-interface tracer depletion and miscible displacement water phase advective tracer methods." Water Resour. Res. **48**:W10519, DOI: 10.1029/2012WR011862.

Kim, H., P. S. C. Rao and M. D. Annable (1997). "Determination of effective air-water interfacial area in partially saturated porous media using surfactant adsorption." Water Resour. Res. **33**:2705-2711.

Kim, H., P. S. C. Rao and M. D. Annable (1999). "Consistency of the interfacial tracer technique: Experimental evaluation." J. Contam. Hydrol. **40**:79-94.

Saripalli, K. P., H. Kim, P. S. C. Rao and M. D. Annable (1997). "Measurement of specific fluid-fluid interfacial areas of immiscible fluids in porous media." Environ. Sci. Technol. **31**:932-936.

Simunek, J., M. Sejna and M. T. van Genuchten (1988). The HYDRUS-1D software pacakage for simulating the one-dimensional movement of water, heat, and multiple solutes in variably-saturated media. Colorado School of Mines, Golden CO, Ground Water Modeling Center.

Simunek, J., M. T. van Genuchten and M. Sejna (2016). "Recent developments and applications of the HYDRUS computer software packages." Vadose Zone J. **15**, DOI: 10.2136/vzj2016.04.0033.

Smith, J. E. and R. W. Gillham (1994). "The effect of concentration-dependent surface tension on the flow of water and transport of dissolved organic compounds: A pressure head-based formulation and numerical model." Water Resour. Res. **30**:343-354.

Smith, J. E. and R. W. Gillham (1999). "Effects of solute concentration-dependent surface tension on unsaturated flow: Laboratory sand column experiments." Water Resour. Res. **35**:973-982.

Tokunaga, T. K., K. R. Olson and J. Wan (2004). "Conditions necessary for capillary hysteresis in porous media: Tests of grain size and surface tension influences." Water Resour. Res. **40**:W05111, DOI: 10.1029/2003WR002908.

Zartman, R. and R. Barsch (1990). "Using surfactant to enhance drainage from a dewatered column." Soil Sci. **149**:52-55.

FIGURE CAPTIONS

Figure 1. Soil water characteristic curves for pure-water wetted and surfactant-wetted sand.

Figure 2. A) Simulated breakthrough curves and **B)** S_W-time relationships for Scenario A (blue in all figures) for systems at initial S_W of 75% and three influent SDBS concentrations. Breakthrough results for the non-reactive tracer (black) and the 0.2 mM SDBS K_D and K_{IW} partitioning test case (red), which do not include surfactant-induced flow, are included for comparison.

Figure 3. A) Simulated breakthrough curves and **B)** S_W-time relationships for SDBS under Scenarios A-D with an initial S_W of ~75% and influent SDBS concentration of 0.2 mM. Simulated breakthrough results for the non-reactive tracer (black) and the 0.2-mM SDBS K_D and K_{IW}-partitioning test case (red), which do not include surfactant-induced flow, are included for comparison. Insets show full simulation time.

Figure 4. Simulated depth profiles for Scenario D of **A)** SDBS concentration; **B)** pressure head; and **C)** water content for multiple time points in a system at initial 75% S_W and 0.2 mM SDBS.

TABLE TITLES

Table 1. Simulation scenarios examined for their effect on surfactant-induced flow and A_I determination, including the conventional SMD setup (Scenario A) and alternative column orientation and column boundary conditions (BCs).

Table 2. Comparison of initial true A_I with the estimated A_I derived from simulated breakthrough curves and initial S_W for Scenarios A and D (0.2 mM SDBS input), expressed as % error. Slight variations in the initial true A_I values for the two scenarios are due to differences in the types of boundary conditions utilized.